Supporting Information

Eichinger and Jentsch 10.1073/pnas.1004248107

SI Materials and Methods

Yeast Strains. Yeast strains used are listed in Table S2. Strains are isogenic to strain SK1 (Y1083, for all meiotic assays), DF5 (Fig. 4*D*), or PJ69-7A (for all yeast two-hybrid assays). Yeast techniques were performed as previously described (1–3). All deletion mutants were constructed by a PCR-based strategy (4, 5) and confirmed by PCR using specific primers. The complete *RED1* ORF, 641 bp of the upstream promoter and 514 bp of its terminator, was cloned into an integrative plasmid (pYIplac211) (6). All *red1* mutant plasmids (pYIplac211 and pGBD-C1) were constructed by site-directed mutagenesis using specific pairs of primers (reverse primers were exactly complementary to the respective forward sequences shown here): $red1^{-mec3}$ ($Q^{537}A$, $V^{540}A$) forward, 5′-cct aag gaa aag cct aat aat gat gca acg gta gcc gga ata acc gaa tta aag tca aat tc-3′; $red1^{-ddc1}$ ($I^{743}A$) forward, 5′-cac aaa caa act tca aga aca agc tta tag ttc aat aaa tca ttt ttc taa c-3′; $red1^{KR}$ forward, 5′-cac tat att tgg gca acc tcc gtc cag gag gca aag aca att cca cag aag gga gag aag gag gca gca gag aag gtt gac aaa ctt tag gcc cat tat cga tg-3′; $red1^{KR1}$ forward, 5′-cta tat ttg ggc aac ctc cgt cca gga ggc aaa gac aat tcc aca gaa ggg aga aaa aga agc agc aga aaa agt tg-3′; and $red1^{KR2}$ forward, 5′-gca aaa aca att cca caa aaa gga gag aag gag gca gca gag aag gtt gac aaa ctt tag gcc cat tat cga tgt ccc ttc c-3′. To compare the phenotypes of different Red1-expressing strains accurately, pYIplac221 plasmids expressing *RED1* WT and mutants under the endogenous promoter were cut by *Afl*II and integrated directly into the *LEU2* locus of the same diploid parental strain. Only diploid strains expressing *RED1* WT and mutants from two copies [confirmed by real-time PCR in comparison to a control locus (*MDV1*) on chromosome X; expression levels were further confirmed by Western blot analysis] were used for phenotypic analysis. The internally GFP-tagged Zip1 construct [obtained from D. Kaback (University of Medicine and Dentistry of New Jersey, Newark, NJ) and described previously (7)] was cut by *Apa*I and integrated into the *URA3* locus. YIplac128-based *pADH1*-^{His}SUMO constructs (*SMT3* ORF N-terminally fused to a 7-histidine tag under a *pADH1* promoter) were integrated into the *URA3* locus by cutting with *EcoR*V, and expression levels were tested by Western blot analysis.

Synchronous Meiotic Time Course. Several colonies of strains grown on selection plates [0.67% yeast nitrogen base (Difco), 0.2% dropout amino acid mix (Difco), 2% (wt/vol) glucose, 2% (wt/vol) agar] for 3 d were inoculated in YPD [1% yeast extract (Difco), 2% (wt/vol) bactopeptone (Difco), 2% (wt/vol) D-(+)-glucose] and cultured overnight at 30 °C, diluted 1:50 in prewarmed yeast bacto peptone acetate media [1% yeast extract (Difco), 2% (wt/vol) bactopeptone (Difco), 2% (wt/vol) potassium acetate], and again cultured overnight at 30 °C. Cells were then harvested (2,000 × *g*, 5 min at room temperature), washed twice with prewarmed water, resuspended in prewarmed 2% potassium acetate media, and cultured under rigorous shaking at 30 °C (flask size at least five times culture volume). Aliquots were removed after the indicated times.

Spore Viability, Germination, and Meiotic Nuclear Division Assays. For spore viability assays, overnight cultures in YPD media were washed four times with prewarmed water and released into sporulation in 1.5% potassium acetate solution for 3 d at room temperature. Samples were digested for 5 min with zymolase (ICN Biochemicals), and tetrads were dissected. Survival of spores on YPD plates was scored after 3 d. For germination assays, spores were isolated and treated with zymolase after 72 h in sporulation media and then plated on YDP plates at 30 °C, as described previously (8). Meiotic (nuclear) divisions were visualized by staining of chromosomal DNA with 1 μg/mL DAPI. For this, samples from synchronously growing cultures were harvested at the indicated times and directly fixed in an equal volume of 100% ethanol for subsequent DAPI staining. Images were recorded and analyzed using a Zeiss Axio Imager Z1 microscope.

Live Cell Microscopy. SC formation was studied essentially by spinning disk microscopy, as described (7). An ANDOR/TiLL iMIC CSU22 spinning disk confocal microscope with a 100× 1.45-N.A. objective lens (Olympus) was used to capture image stacks of 250-nm step-size. Yeast cells were released into synchronous sporulation, and samples were taken at the respective time point, directly mounted onto Con A-coated glass-bottomed dishes (MatTek), and immediately observed under the microscope. After taking a bright-field picture to count the total number of cells in the respective fields, several stacks of the Zip1-GFP fusion signal were monitored. For data analysis, maturation of SC was categorized into five classes: early stage, diffuse, dot-like, pre-SCs, and full SCs (Fig. S3). For quantitative assays, only pre-SCs and full SCs were distinguished and counted. In each of five to six independent experiments, more than 100 cells were analyzed for each time point. The mean values are indicated in each figure.

Protein Techniques and Antibodies. Yeast protein extracts, analytical denaturing Ni-NTA pull-downs, and isolation of SUMO-conjugates were done as described (1, 2, 9). For yeast two-hybrid assays, PJ69-7A cells [derivatives of strains described by James et al. (10)] were transformed with the respective activating domain- or binding domain-fusion constructs [respective ORFs were PCR-amplified and cloned into pGAD-C1 or pGBD-C1 plasmids using an appropriate pair of restriction enzymes (10) and spotted on −His plates ($SC^{-leu-trp-his}$) plates for selection or control plates ($SC^{-leu-trp}$)]. For SDS/PAGE, commercial 4–12% (wt/vol) gradient gel systems (Invitrogen) were used. Gels were run using a Mops buffer (50 mM Tris base, 50 mM Mops, 0.1% SDS, 1 mM EDTA) and blotted on PVDF membranes (Immobilon-P; Millipore) by standard methods for subsequent Western blot analysis. For this, antibodies against Red1 (1:1,000, this study), Zip1 (1:1,000; provided by M. Knop, European Molecular Biology Laboratory, Heidelberg, Germany), Rad52 (1), histone H2A-S129 phosphorylation (1:10,000; Upstate, according to manufacturer's protocol) and Pgk1 (1:5,000, Molecular Probes) were used. Antibodies against yeast Red1 were raised against two Red1 peptides (peptide sequence 1: H_2N-CDR SVS IRS DEW DLK S-$CONH_2$ and peptide sequence 2: H_2N-CRT DKK VTG EKS SPE T-$CONH_2$; Eurogentec) and affinity-purified using these peptides using the SulfoLink Coupling Gel method (Pierce). Peroxidase-coupled secondary antibodies were applied at a 1:5,000 dilution and detected by an Amersham ECL detection system (GE Healthcare).

1. Sacher M, Pfander B, Hoege C, Jentsch S (2006) Control of Rad52 recombination activity by double-strand break-induced SUMO modification. *Nat Cell Biol* 8: 1284–1290.

2. Hoege C, Pfander B, Moldovan GL, Pyrowolakis G, Jentsch S (2002) RAD6-dependent DNA repair is linked to modification of PCNA by ubiquitin and SUMO. *Nature* 419: 135–141.

3. Pfander B, Moldovan GL, Sacher M, Hoege C, Jentsch S (2005) SUMO-modified PCNA recruits Srs2 to prevent recombination during S phase. *Nature* 436:428–433.
4. Knop M, et al. (1999) Epitope tagging of yeast genes using a PCR-based strategy: More tags and improved practical routines. *Yeast* 15 (10B):963–972.
5. Janke C, et al. (2004) A versatile toolbox for PCR-based tagging of yeast genes: New fluorescent proteins, more markers and promoter substitution cassettes. *Yeast* 21:947–962.
6. Gietz RD, Sugino A (1988) New yeast-Escherichia coli shuttle vectors constructed with in vitro mutagenized yeast genes lacking six-base pair restriction sites. *Gene* 74:527–534.
7. Scherthan H, et al. (2007) Chromosome mobility during meiotic prophase in Saccharomyces cerevisiae. *Proc Natl Acad Sci USA* 104:16934–16939.
8. Herman PK, Rine J (1997) Yeast spore germination: A requirement for Ras protein activity during re-entry into the cell cycle. *EMBO J* 16:6171–6181.
9. Sacher M, Pfander B, Jentsch S (2005) Identification of SUMO-protein conjugates. *Methods Enzymol* 399:392–404.
10. James P, Halladay J, Craig EA (1996) Genomic libraries and a host strain designed for highly efficient two-hybrid selection in yeast. *Genetics* 144:1425–1436.

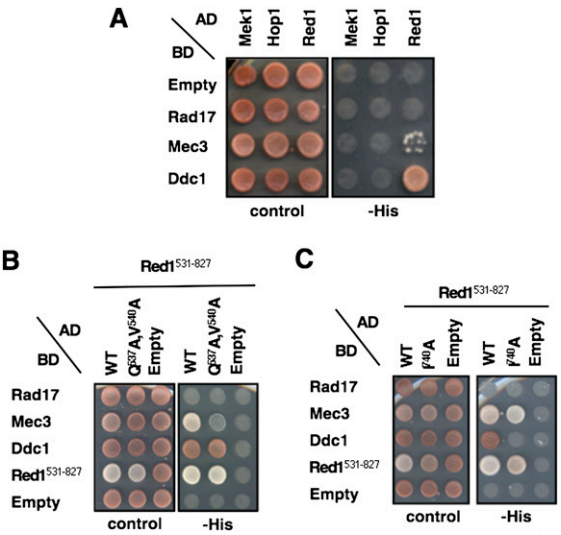

Fig. S1. (*A*) Meiotic protein Red1 (but not Hop1 and Mek1) interacts with the 9-1-1 complex. Two-hybrid interactions identified on selective media (*Right*, −His) of fusions of full-length proteins with the Gal4 activating domain (AD) or DNA binding domain (BD) are shown. Two-hybrid interactions to Red1 are stronger if C-terminal Red1 fragments are used (Fig. 1). (*B*) 9-1-1 binding-deficient Red1^{-Mec3} does not bind to Mec3 but is proficient in Ddc1 and Red1 interaction. (*C*) 9-1-1 binding-deficient Red1^{-Ddc1} does not bind to Ddc1 but is proficient in Mec3 and Red1 interaction. Two-hybrid interactions identified on selective media (*Right*, −His) of fusions of Red1 C-terminal proteins (amino acids 531–827) and full-length 9-1-1 subunits with the Gal4 AD or DNA BD are shown. The white colony color is indicative of better growth. Images were taken after 3 d at 30 °C.

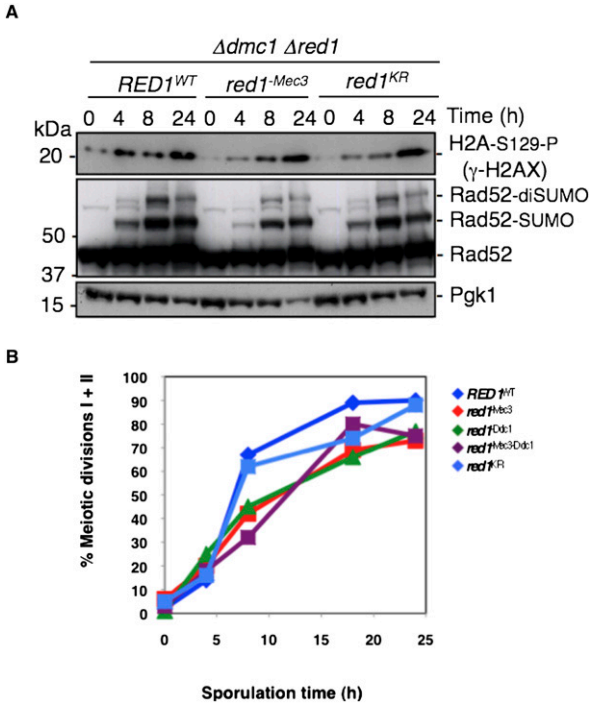

Fig. S2. (*A*) *red1*^{KR} and *red1*$^{-Mec3}$ mutants sustain robust checkpoint arrest in a Δ*dmc1* strain similar to *RED1*^{WT}. Extracts of synchronously sporulating cells were made at the indicated times and probed by Western blot analysis for phosphorylated H2A (equivalent to mammalian γ-H2AX) and Rad52 SUMOylation as measures for checkpoint activation as well as for Pgk1. Here, the strains CE453 (*RED1*^{WT}), CE454 (*red1*$^{-Mec3}$), and CE455 (*red1*^{KR}) were used. Complete genotypes are provided in Table S2. (*B*) Meiotic nuclear divisions of Red1 alleles. Meiotic (nuclear) divisions were monitored by DAPI staining of chromosomal DNA. Samples from synchronously growing cultures were harvested at the indicated times and fixed in ethanol for subsequent DAPI staining. Here, the strains CE774 (*RED1*^{WT}), CE775 (*red1*$^{-Mec3}$), CE776 (*red1*$^{-Ddc1}$), CE777 (*red1*$^{-Mec3,-Ddc1}$), and CE778 (*red1*^{KR}) were used. Complete genotypes are provided in Table S2.

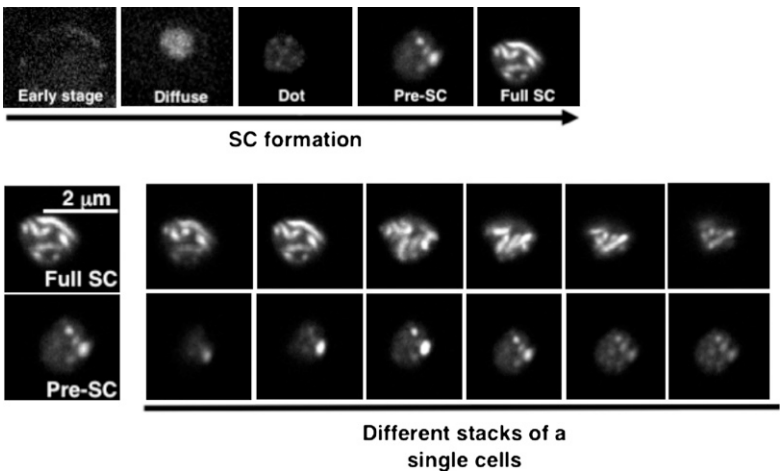

Fig. S3. Stepwise SC formation in sporulating diploid cells. In each experiment, GFP-tagged Zip1 was directly visualized using spinning disk microscopy in five to six independent experiments. For each time point, 100 cells were captured and several stacks were visualized. Using this method, the events in live cells at specific time points were immediately monitored without major technical preparations, thereby allowing a clear distinction between pre-SCs and full SC formation. Here, cells of CE774 (*RED1*^{WT}) strains at different sporulation stages are shown.

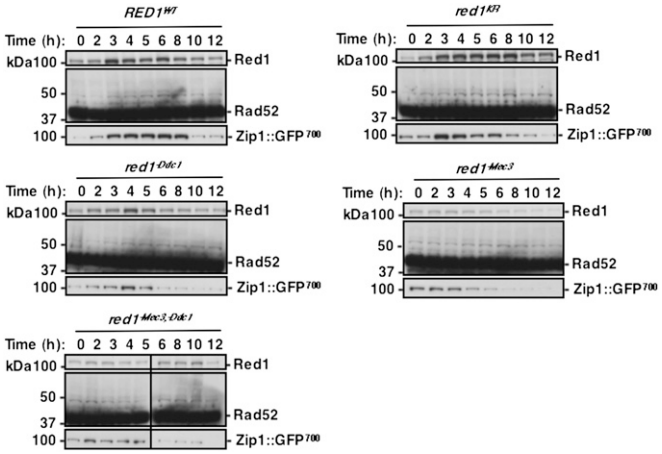

Fig. S4. Levels of meiotic proteins. Expression of Red1 variants, Zip1, and Rad52 during meiotic progression is shown. Strains were released into synchronous sporulation, and extracts were prepared at the indicated time points and analyzed by Western blotting using antibodies against Red1, Zip1, and Rad52. Here, the strains CE774 (*RED1*^{WT}), CE775 (*red1*$^{-Mec3}$), CE776 (*red1*$^{-Ddc1}$), CE777 (*red1*$^{-Mec3,-Ddc1}$), and CE778 (*red1*^{KR}) were used. Complete genotypes are provided in Table S2.

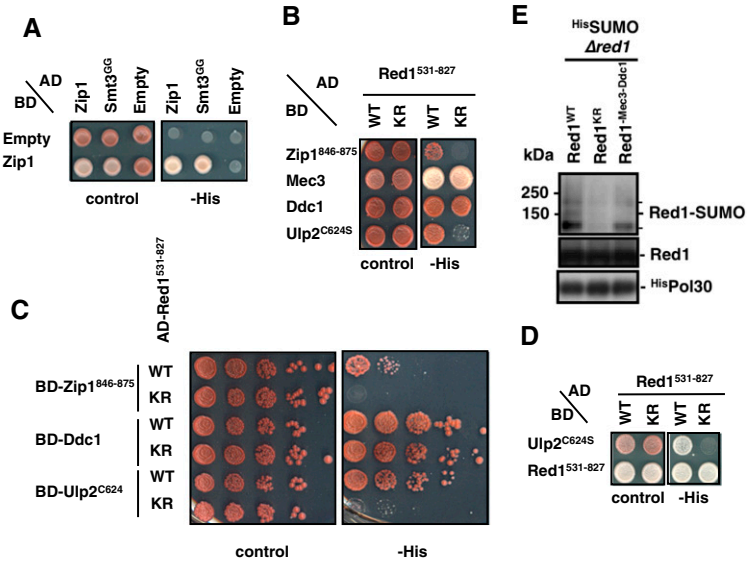

Fig. S5. Interaction profile of the SUMOylation-deficient Red1^{KR} mutant. (*A*) Zip1 interacts with Zip1 and SUMO in a two-hybrid assay. (*B*) Red1^{KR} (amino acids 531–827) is deficient in binding Zip1$^{846–875}$ and Ulp2^{C624S} but associates normally with the 9-1-1 subunits Mec3 and Ddc1. (*Right*) Two-hybrid interactions identified on selective media (−His) of fusions with activating domain (AD) or DNA binding domain (BD) are shown. The white colony color is indicative of better growth. Images were taken after 5 d at 30 °C. (*C*) Red1^{KR} interactions were done as in *B* but spotted as 1:10 serial dilutions. (*D*) Enzymatic inactive Ulp2 (Ulp2^{C624S}) specifically binds SUMOylation-proficient Red1 but not the SUMOylation-deficient Red1^{KR} variant. (*E*) SUMOylation of a Red1 variant deficient in 9-1-1 binding. 9-1-1 binding to Red1 has no significant influence on Red1 SUMOylation. Diploid homozygous SK1 Δ*red1* deletion strains with integrated genes encoding ^{His}SUMO (expression by *ADH1* promoter, CE382) and a Red1 variant deficient in 9-1-1 binding (Red1$^{-Mec3,-Ddc1}$) were released into synchronous sporulation. SUMO-conjugates were isolated by Ni-NTA pull-down after 8 h and detected by Western blotting using an anti-Red1 antibody. Samples from separate ^{His}Pol30-expressing cultures were added to control for pull-down efficiency. The SUMOylation-deficient Red1^{KR} variant was used as a negative control (*Middle*, Red1 input levels). Strains used were CE659 (*RED1*^{WT}), CE662 (*red1*^{KR}), and CE663 (*red1*$^{-Mec3-Ddc1}$). Complete genotypes are provided in Table S2.

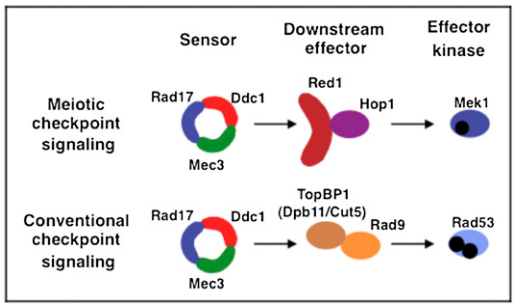

Fig. S6. Analogy of Red1 and TopBP1 (Dpb11/Cut5) in checkpoint signaling. (*Lower*) In the conventional DNA damage checkpoint, 9-1-1 associates with TopBP1 (Dpb11/Cut5) via its Ddc1 subunit. This binding (in *S. cerevisiae*, often in complex with Rad9) transduces the signal to the effector kinase Rad53. (*Upper*) In the meiotic pathway, which governs Spo11-induced DSBs, 9-1-1 binds Red1. Ddc1-Red1 interaction is required for transmitting the signal to the dedicated meiotic checkpoint kinase Mek1. The forkhead-associated domains of Mek1 and Rad53 are shown in black.

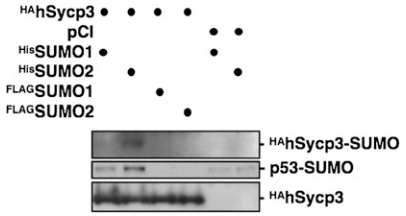

Fig. S7. Human Sycp3 is modified with SUMO. HA-tagged human Sycp3 (^{HA}hSycp3, a putative Red1 homolog) and human ^{His}SUMO1 or ^{His}SUMO2 were overexpressed in HEK 293T cells. SUMO conjugates were isolated by Ni-NTA pull-downs, and modified species of Sycp3 were detected by Western blot analysis using a monoclonal anti-HA antibody (clone 16B12; Convance). Modification of Sycp3 occurred specifically with ^{His}SUMO2, barely with ^{His}SUMO1, but not in controls (expression of vector pCI or of ^{FLAG}SUMO1 and ^{FLAG}SUMO2, which lack His-tags). SUMOylation of endogenous p53 was detected by a monoclonal anti-p53 antibody (DO-1; Santa Cruz) and used as a positive control (*Bottom*, ^{HA}hSycp3 input levels).

Table S1. Spore viabilities

Genotype	% Spore viability (no. spores counted)
Group A	
WT (Y1083)	96.7% (152)
RED1^{WT} ZIP1-GFP	87.8% (140)
red1^{-Mec3} ZIP1-GFP	79.2% (140)
red1^{-Ddc1} ZIP1-GFP	5.7% (140)
red1$^{-Mec3,-Ddc1}$ ZIP1-GFP	7.1% (140)
red1^{KR} ZIP1-GFP	39% (100)
Δ*zip1*	28.3% (148)
Δ*zip3*	10% (40)
Group B	
WT (Y1083)	96.7% (152)
RED1^{WT} *pADH*-^{His}SUMO	93.7% (64)
red1^{-Mec3} *pADH*-^{His}SUMO	84.4% (64)
red1^{-Ddc1} *pADH*-^{His}SUMO	20.3% (64)
Δ*rad17*	22.5% (40)
Δ*mec3*	25% (40)
Δ*ddc1*	10% (40)

Group A: WT cells (SK1 strain Y1083) were compared with Zip1-GFP–expressing cells that express Red1 WT and 9-1-1 binding-deficient or SUMOylation-deficient Red1 variants (*red1*$^{-Mec3}$, *red1*$^{-Ddc1}$, *red1*$^{-Mec3,-Ddc1}$, and *red1*^{KR} strains: Y1083, CE774, CE775, CE776, CE777, and CE778; complete genotypes are provided in Table S2). Strains were released into sporulation in 1.5% (wt/vol) potassium acetate solution for 3 d before tetrade dissection, and spore viability was scored on YPD plates after 3 d. Indicated are the percentages of viable spores and the total number of spores counted (in parentheses). Also shown are spore viabilities of Δ*zip1* (Y2109) and Δ*zip3* (CE522) mutants. Group B: Spore viability of *red1* mutants and 9-1-1 deletion strains. WT cells (Y1083) were compared with Red1 WT or 9-1-1 binding-deficient mutants (*red1*$^{-Mec3}$, *red1*$^{-Ddc1}$). Also shown are spore viabilities of 9-1-1 deletion strains (Δ*rad17,* Δ*mec3,* and Δ*ddc1*). Strains were released into sporulation in 1.5% potassium acetate solution for 3 d before tetrade dissection, and spore viability was scored on YPD plates after 3 d. Indicated are the percentages of viable spores and the total number of spores counted (in parentheses). Strains were used in this order: Y1083 (WT), CE640 (*RED1*^{WT}), CE643 (*red1*$^{-Mec3}$), CE646 (*red1*$^{-Ddc1}$), CE525 (Δ*rad17*), CE528 (Δ*mec3*), and CE531 (Δ*ddc1*). Complete genotypes are provided in Table S2.

Table S2. List of the yeast strains used in this study

Strain	Genotype	Source
DF5	*his3Δ200, leu2-3,11, lys2-801, trp1-1, ura3-52*	1
Y1094	*DF5, SMT3::pYI-pADH1-^{His}SMT3::URA3*	This study
Y1083	*ho::hisG/ho::hisG, lys2/lys2, ura3/ura3, leu2/ leu2, his3/ his3, trp1-ΔFA/ trp1-ΔFA*	2
CE382	*SK1, URA3::pYI-pADH1-^{His}SMT3*	This study
CE387	*SK1, red1::kanMX6/red1::kanMX6, URA3::pYI-pADH1-^{His}SMT3*	This study
CE659	*SK1, red1::kanMX6/red1::kanMX6, URA3::pYI-pADH1-^{His}SMT3, LEU2::pYI-RED1^{WT}/LEU2::pYI-RED1^{WT}*	This study
CE662	*SK1, red1::kanMX6/red1::kanMX6, URA3::pYI-pADH1-^{His}SMT3, LEU2::pYI-red1^{KR}/LEU2::pYI-red1^{KR}*	This study
CE663	*SK1, red1::kanMX6/red1::kanMX6, URA3::pYI-pADH1-^{His}SMT3, LEU2::pYI-red1$^{-Mec3,-Ddc1}$/LEU2::pYI-red1$^{-Mec3,-Ddc1}$*	This study
CE774	*SK1, red1::kanMX6/red1::kanMX6, zip1::natNT2/zip1::natNT2, URA3::pYI-ZIP1::GFP^{700}, LEU2::pYI-RED1^{WT}/LEU2::pYI-RED1^{WT}*	This study
CE775	*SK1, red1::kanMX6/red1::kanMX6, zip1::natNT2/zip1::natNT2, URA3::pYI-ZIP1::GFP^{700}, LEU2::pYI-red1^{-Mec3}/LEU2::pYI-red1^{-Mec3}*	This study
CE776	*SK1, red1::kanMX6/red1::kanMX6, zip1::natNT2/zip1::natNT2, URA3::pYI-ZIP1::GFP^{700}, LEU2::pYI-red1^{-Ddc1}/LEU2::pYI-red1^{-Ddc1}*	This study
CE777	*SK1, red1::kanMX6/red1::kanMX6, zip1::natNT2/zip1::natNT2, URA3::pYI-ZIP1::GFP^{700}, LEU2::pYI-red1$^{-Mec3,-Ddc1}$/LEU2::pYI-red1$^{-Mec3,-Ddc1}$*	This study
CE778	*SK1, red1::kanMX6/red1::kanMX6, zip1::natNT2/zip1::natNT2, URA3::pYI-ZIP1::GFP^{700}, LEU2::pYI-red1^{KR}/LEU2::pYI-red1^{KR}*	This study
CE525	*SK1, rad17::natNT2/rad17::natNT2*	This study
CE528	*SK1, mec3::natNT2/mec3::natNT2*	This study
CE531	*SK1, ddc1::natNT2/ddc1::natNT2*	This study
CE522	*SK1, zip3::natNT2/zip3::natNT2*	This study
Y2109	*SK1, zip1::kanMX6/zip1::kanMX6*	This study
CE566	*SK1, zip3::natNT2/zip3::natNT2URA3::pYI-pADH1-^{His}SMT3*	This study
Y2031	*SK1, dmc1::HIS3MX6/dmc1::HIS3MX6, red1::kanMX6/red1::kanMX6*	3
CE571	*SK1, dmc1::HIS3MX6/dmc1::HIS3MX6, red1::kanMX6/red1::kanMX6, LEU2::pYI-RED1^{WT}*	This study
CE579	*SK1, dmc1::HIS3MX6/dmc1::HIS3MX6, red1::kanMX6/red1::kanMX6, LEU2::pYI-red1^{-Ddc1}*	This study
CE640	*SK1, red1::kanMX6/red1::kanMX6, URA3::pYI-pADH1-^{His}SMT3, LEU2::pYI-RED1^{WT}/LEU2::pYI-RED1^{WT}*	This study
CE643	*SK1, red1::kanMX6/red1::kanMX6, URA3::pYI-pADH1-^{His}SMT3, LEU2::pYI-red1^{-Mec3}/LEU2::pYI-red1^{-Mec3}*	This study
CE646	*SK1, red1::kanMX6/red1::kanMX6, URA3::pYI-pADH1-^{His}SMT3, LEU2::pYI-red1^{-Ddc1}/LEU2::pYI-red1^{-Ddc1}*	This study
CE453	*SK1, dmc1::HIS3MX6/dmc1::HIS3MX6, red1::kanMX6/red1::kanMX6, LEU2::pYI-RED1^{WT}/LEU2::pYI-RED1^{WT}*	This study
CE454	*SK1, dmc1::HIS3MX6/dmc1::HIS3MX6, red1::kanMX6/red1::kanMX6, LEU2::pYI-RED1^{-Mec3}/LEU2::pYI-RED1^{-Mec3}*	This study
CE455	*SK1, dmc1::HIS3MX6/dmc1::HIS3MX6, red1::kanMX6/red1::kanMX6, LEU2::pYI-RED1^{KR}/LEU2::pYI-RED1^{KR}*	This study
PJ69-7A	*trp901-, leu2-3,112, ura3-53, his3-200, gal4, gal80, GAL1::HIS3, GAL2-ADE2, met2::GAL7-lacZ*	4

1. Finley D, Ozkaynak E, Varshavsky A (1987) The yeast polyubiquitin gene is essential for resistance to high temperatures, starvation, and other stresses. *Cell* 48:1035–1046.
2. Gasior SL, Wong AK, Kora Y, Shinohara A, Bishop DK (1998) Rad52 associates with RPA and functions with rad55 and rad57 to assemble meiotic recombination complexes. *Genes Dev* 12:2208–2221.
3. Sacher M, Pfander B, Hoege C, Jentsch S (2006) Control of Rad52 recombination activity by double-strand break-induced SUMO modification. *Nat Cell Biol* 8:1284–1290.
4. James P, Halladay J, Craig EA (1996) Genomic libraries and a host strain designed for highly efficient two-hybrid selection in yeast. *Genetics* 144:1425–1436.